OPEN ACCESS

An optimized kHz two-colour high harmonic source for seeding free-electron lasers and plasma-based soft x-ray lasers

New Journal of Physics
The open-access journal for physics

An optimized kHz two-colour high harmonic source for seeding free-electron lasers and plasma-based soft x-ray lasers

G Lambert[1,4], J Gautier[1], C P Hauri[2], Ph Zeitoun[1], C Valentin[1], T Marchenko[1], F Tissandier[1], J Ph Goddet[1], M Ribiere[1], G Rey[1], M Fajardo[3] and S Sebban[1]

[1] Laboratoire d'Optique Appliquée, ENSTA-CNRS-École Polytechnique, Chemin de la Hunière, 91761 Palaiseau, France
[2] Paul Scherrer Institute, 5232 Villigen, Switzerland
[3] Centro de Física dos Plasmas/Instituto Superior Técnico, Av. Rovisco Pais, 1049-001 Lisboa, Portugal
E-mail: guillaume.lambert@ensta.fr

New Journal of Physics **11** (2009) 083033 (17pp)
Received 31 March 2009
Published 28 August 2009
Online at http://www.njp.org/
doi:10.1088/1367-2630/11/8/083033

Abstract. Free-electron lasers (FEL) and plasma-based soft x-ray lasers (PSXL) have been recently evolving very fast from the vacuum ultraviolet to the soft x-ray region. Once seeded with high harmonics, these schemes are considered as the next generation soft x-ray light sources delivering ultrashort pulses with high temporal and spatial coherence. Here, we present a detailed experimental study of a kHz two-colour high harmonic generation performed in various gases and investigate its potential as a suitable evolution of the actual seeding sources. It turns out that this double harmonic content source is highly tuneable, controllable and delivers intense radiation (measured here with a calibrated photodiode) with only one order of magnitude difference in the photon yield from 65 to 13 nm. Then, first and foremost, injections could be achieved at wavelengths shorter than what was previously accessible in FEL and PSXL and/or additional energy could be extracted. Also, such a strong and handy seed could allow the saturation range of FEL devices to be greatly extended to shorter wavelengths and would bring higher spectral as well as intensity stabilities in this spectral zone.

[4] Author to whom any correspondence should be addressed.

Contents

1. Introduction

Seeding plasma-based soft x-ray lasers (PSXL) [1]–[6] and free-electron lasers (FEL) [7, 8] with high-order harmonics (HH) generated in gas from the vacuum ultraviolet (VUV, ≈80–130 nm) to the soft x-ray (≈10–40 nm) region is a quite recent but emerging topic. Indeed, it has already opened significant perspectives for developing the ultimate future relatively compact coherent jitter-free and aberration-free source, in order to observe the ultrafast dynamics of matter at the nanometre scale. Although seeding was originally employed for different motivations in FEL and PSXL, in both cases it relies on benefits from the high-quality properties of the HH source, particularly the ultrashort pulse duration or the high degree of spatial and temporal coherence [9, 10]. On the other hand, seeding can help to overcome the main HH limitation, the relatively low peak power for single shot applications.

The first highly successful seeding experiment in a PSXL was performed in 2000 at 32.8 nm in a Ni-like Kr optical field ionized (OFI) amplifier [1]. Before that, in all the PSXL operating at saturation, population inversion between the levels of the lasing ion was induced by electron collisional excitation in a single pass, providing a high gain value at short wavelength in an amplified spontaneous emission (ASE). Yet, this radiation was characterized by a long pulse duration, an inhomogeneous beam profile and a low spatial coherence.

In the seeding configuration of PSXL, the injected beam acts as an 'oscillator' for a classical laser chain, leading to the generation of a high optical spatial quality beam, which is amplified while propagating through the population inverted plasma column. This relatively compact device then combines the production of an intense emission, due to the high energy extracted from the plasma amplifier (sub-microjoule), to the high optical spatial quality of the harmonic beam [4]. More recently, seeding of PSXL was also carried out in more dense plasmas than in the OFI scheme, in order to obtain higher saturation and broader spectral linewidth for reaching shorter pulse durations in the femtosecond scale (limited to picoseconds nowadays). These plasmas are created from solid targets, either Ne-like (Mn [2] and Ti [3] at, respectively, 26.9 and 32.6 nm) or Ni-like (Mo [5], Ag [5] and Cd [6] at 18.9, 13.9 and 13.2 nm) ions.

Since the beginning of this century, novel linear accelerator-based single-pass FEL sources have been emerging around the world. Presently, different sites have implemented or plan to implement soon seeding schemes in their facilities as a main mode of functioning. The first proof-of-principle seeding experiment was conducted in 2007 at 160 nm [8] at the SCSS (SPring-8 Compact SASE Source, Japan) Test Accelerator [11]. The next scheduled

test-bed HH seeding facility is SPARC (Sorgente Pulsata e Amplificata di Radiazione Coerente, Italy) [12], which is almost ready to deliver photons in the VUV region down to 114 nm. sFLASH (seeded Free-electron LASer of Hamburg) [13, 14] is also now being designed and should operate in 2010 in the soft x-ray region from 30 to 13 nm. FERMI (Italy) [15] and MAX-IV (Sweden) [16] FELs also expect to use 20–30 nm HH sources for seeding. Other projects, such as SPARX (1.5 nm, Italy) [17], ARC-EN-CIEL (0.8 nm, France) [18] and PSI-XFEL (0.1 nm, Switzerland) [19] consider seeding as a valuable option for x-rays. In these proposals, some additional amplification stages of FEL harmonics of the seed, like in high-gain harmonic-generation (HGHG) [20] and cascade [21, 22] configurations, will be coupled to the soft x-ray seed injection.

Essentially, the seeding configuration in FEL is a direct evolution of the classical self-amplified spontaneous emission (SASE) [23, 24], which provides a very high brightness emission (maximum of 100 μJ in pulses of less than 100 fs duration) at short wavelengths but with a limited temporal coherence. The spectral and temporal profiles are typically composed of a series of randomly distributed spikes, reflecting the stochastic nature of the SASE generation process that is the amplification of noise. In seeding arrangements, the amplification is triggered by the strong harmonic seed rather than the noise floor, leading to strong and coherent amplified FEL radiation. The proof-of-principle experiment showed that the 160 nm light could be coherently amplified, while the seeded energy per pulse was of the order of a nanojoule [8]. The single shot seeded emission then achieved three orders of magnitude higher intensity than the unseeded one and a factor of 500 compared to the seed, almost reaching the microjoule level. Moreover, the corresponding spectral distribution presented a regular quasi-perfect Gaussian shape.

As most of the applications aim at the wavelength range from soft x-ray to x-ray ($<$10 nm), valuable HH seed intensity is required in this spectral range, where unluckily the efficiency of the classical harmonic generation, from an 800 nm Ti:Sa laser system, has a sharp decrease. In addition, for seeding an FEL, the injected peak power must overcome the electron beam shot noise, which is inversely proportional to the wavelength of emission [25]. Finally, seeding with high harmonics should not have any constraint on the machine performance, such as the repetition rate and the tuneability. This is why there is an urgent need for developing new HH sources, more intense at shorter wavelengths, with higher repetition rates, larger tuneability, and with an easy control of the injection parameters (mainly wavelength, intensity and pulse duration).

One of the solutions could be the use of a 1.2–1.5 μm parametric amplifier [26] in order to get a viable continuously tuneable seed source in the soft x-ray region. Indeed, as this involves working with a higher fundamental wavelength (compared to an 800 nm Ti:Sa laser), the maximum of the emission is blueshifted (equations (2) and (3)) and lower wavelengths can be reached. Yet, the efficiency of generation is, in this case, rather weak, and as a consequence it strongly limits the feasibility of seeding with such a technique.

Recently, a Korean team observed in an orthogonally polarized two-colour laser field technique [27], consisting of mixing the fundamental frequency (ω, actually the fundamental pulsation) and its second harmonic (2ω) generated in a beta barium borate (BBO, type 1) crystal, a strong enhancement of the harmonic generation efficiency in a helium gas jet [28] at 21.6 nm and with a 10 Hz Ti:Sa laser. The increase has been explained using the so-called semiclassical three-step model (free electrons tunnelled from the gas atom, oscillating in the laser field and which can be recombined with the atom core in a radiative process); the

two-colour laser field induces a selection of the short electron quantum path, for which the specific moment when the electrons are released from the atom corresponds to a 10 times higher ionization rate than with the single-colour field [29].

We present here a detailed experimental study of this method applied to a kHz laser system. Our frequency doubling geometric configuration is more straightforward than the Koreans' one [28], where the phase difference induced by the BBO crystal between ω and 2ω was controlled via the addition of a silicate plate on both beam paths. In our case, we do not use the commonly used plate since we did not observe in our experimental conditions any additional significant increase of the HH yield. Moreover, as this component has to be placed between the BBO crystal and the gas medium, the laser dimensions are small at this position, causing long-term damage to the plate surface due to the kHz repetition rate and thus strongly limiting the efficiency of the harmonic generation process. As a result, our proposed setup is very simple and can be easily implemented in HH seeding schemes.

A series of spectra has been obtained in the range from 65 nm down to 17 nm using diverse gases for generation and also different optimization parameters compared to the ones used for ω. It mainly showed a higher efficiency for He and Ne gases generating at shorter wavelengths and a significant control of the harmonic intensity for specific orders via the gas pressure, the gas cell length and the intensity of the 2ω component. In summary, this two-colour experiment should fulfil all the above-mentioned seeding requirements for PSXL and FEL.

Finally, based on numerical simulations, realistic harmonic seeding experiments which could be performed on the SCSS Test Accelerator (the only actual HH seeded FEL in operation) at wavelengths shorter than 55 nm is presented. This value corresponds to the fundamental wavelength limit, below which the full saturation is no longer reached in the SASE mode. Seeding with an intense seed beam, obtained in the two-colour configuration, would then allow the saturation to be extended towards the soft x-ray region. In combination with the possibility of controlling the high harmonic spectra with the two-colour technique (maximum of intensity at the desired wavelength), this seeding will provide users with much more stable light, not only at the designed FEL wavelength for the SASE mode but also within a much larger wavelength range.

2. Experimental considerations

The two-colour ($\omega + 2\omega$) harmonic generation experiment was performed at the Laboratoire d'Optique Appliquée (France) by means of a kHz Ti:Sa laser system at 800 nm (ω), delivering a maximum of 7 mJ energy in 35 fs full-width at half-maximum (FWHM) pulses. Figure 1(a) presents a scheme of the setup. In order to generate the 400 nm radiation (2ω), a BBO (type 1) doubling crystal, is directly inserted in the infrared (IR) beam path between a 1.5 m focusing lens and a gas cell (typically 4–7 mm long). In this geometry, the second harmonic component propagates along the same axis as the IR beam, and consequently the spatial overlap between the ω and 2ω parts is automatically achieved in the active medium. Moreover, the polarization of the second harmonic is perpendicular to the polarization of the fundamental frequency, which corresponds to the situation of the most efficient harmonics generation, according to latest results [28].

Due to the group velocity mismatch between ω and 2ω in the nonlinear crystal, the IR beam is delayed (18.7 fs for 100 μm thick BBO) compared to the blue beam (figure 1(b)). Also, this latter beam can get a longer pulse duration, approximately equal to the induced delay plus

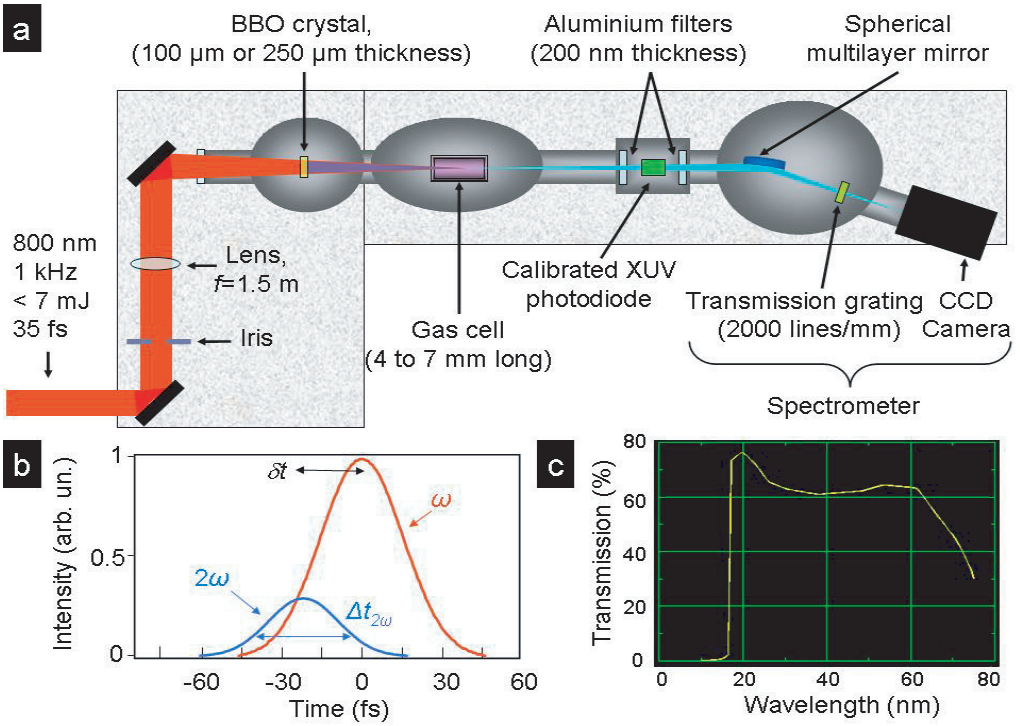

Figure 1. (a) Layout of the kHz two-colour high harmonic generation experiment with a BBO crystal inserted directly in the IR beam path. f is the focal length of the lens used for generating harmonics. (b) Schematic intensity profile in the time domain of ω and 2ω components after passing through the 100 μm thickness doubling-frequency crystal. δt is the temporal shift between ω and 2ω induced by the group velocity mismatch in the nonlinear crystal. $\Delta t_{2\omega}$ is the pulse duration of the 2ω component. (c) Typical transmission of a pure aluminium filter in the VUV to the soft x-ray range, calculated from the centre for x-ray optics (CXRO) website [30] with 200 nm of Al thickness.

a certain percentage ($\approx$50%) of the IR beam pulse duration, as the energy of this latter beam is in general not high enough in the pulse wings to generate the 400 nm emission. To be more specific, the pulse duration should be estimated with the following typical law:

$$\Delta t_{2\omega} \approx \sqrt{\delta t^2 + \frac{(\Delta t_\omega)^2}{2}}. \tag{1}$$

While for a 100 μm thick BBO the pulse duration should be close to the fundamental one ($\approx$30–35 fs FWHM), for a 250 μm thick BBO it should attain about 50–55 fs FWHM. As a consequence, in our particular geometrical configuration where no control of the phase and delay between the two beams can be performed, the 2ω component first arrives in the gas cell and the temporal overlap is not optimized. In general, the thicker the crystal, the higher the 2ω component intensity but the smaller the temporal overlap. This explains why we limit the BBO thickness to 250 μm, which seems to be, however, thick enough for the purpose of the experiment. Also, as previously mentioned, the addition of a well-chosen silicate plate in our experimental conditions did not bring about any further increase of the HH flux. For a shorter

fundamental pulse duration and/or a thicker BBO crystal, the addition of a silicate plate must be reconsidered.

Actually, the other basic parameters characterizing the generation in a two-colour configuration, such as the intensities of the fundamental and blue beams at the generating position in the cell, and the real gas pressure inside the cell, are difficult to evaluate.

For instance, if the available energy of the IR laser delivered by the Ti:Sa system at the exit of the compressor and contained in the full aperture beam ($\phi = 40$ mm in $1/e^2$) is well known (E_ω), the actual value of the energy used is quite low mainly due to an important number of optical components placed in the IR laser path. Moreover, the laser intensity corresponding to the position of generation in the gas cell (I_ω) is lower than the one deduced from the parameters provided at first. Indeed, the IR beam is focused some millimetres after the centre of the gas cell for optimizing the process of generation, giving a quite larger focal spot at the central position of the gas cell. Then, in order to quantify both fundamental and second harmonic intensities (I_ω and $I_{2\omega}$, respectively), one has to first consider the generation efficiency of the crystal for producing the blue beam. One can consider typical values of 25 and 35% for a 100 and 250 μm thick BBO, respectively. Secondly, as for perfectly Gaussian beams, the 400 nm spatial beam profile at the doubling crystal location would be proportional to the square of the intensity profile of the 800 nm beam, the focal spot of the 2ω diffraction-limited beam would have a size 1.414 ($\sqrt{800/400}$) times smaller than the fundamental. Thirdly, in a $\omega + 2\omega$ process, the harmonics are generated in the region where both beams are superposed, that is, in our configuration, in the focusing region of the blue beam. As a consequence, the intensity of the IR beam considered for the generation is about 15% smaller than that of the total intensity. Finally, for gases that can be easily ionized, like argon, the harmonic yield can be maximized by clipping the IR beam with an iris (figure 1(a)), changing both energy (decrease) and waist (increase). In this well-established technique [31], a compromise is performed between considerations of focal geometry and ionization for small apertures and harmonic dipole amplitude and phase for large apertures. For all these reasons, values of I_ω and $I_{2\omega}$ which will be provided in the caption of figures are only estimations of the intensities corresponding to the position of generation in the gas cell (not to the focusing position) and are based on all these above-mentioned statements and not on measurements.

Also, P_G represents the pressure measured at the exit of a controllable valve, which regulates the amount of pressure to be delivered and which is placed far from the gas cell, and is clearly not the real pressure inside the gas cell, but its upper limit.

The system for detecting the harmonic intensity content is based on a spectrometer composed of a spherical mirror at grazing incidence (15°) with 800 nm anti-reflection coating (ZrO_2/Si multilayer deposit), a transmission grating (2000 lines mm^{-1} with a flat diffraction efficiency as a function of the wavelength in the presented spectral range) and a CCD camera (Princeton, 1340 × 400 pixels, 20 × 20 μm^2). From the recorded pictures (vertical position as a function of the wavelength), spectra are obtained by cuts in the horizontal plan and by the integration of this cut over the vertical dimension. Finally, they can be calibrated in absolute energy per pulse by means of a solarblind XUV photodiode (from NIST laboratory). Two thin aluminium filters (≈200 nm thickness each) prevent the IR beam from propagating to the spectrometer, but unfortunately also attenuate the HH photon flux. From 65 to 17 nm, the filter transmission assuming pure aluminium is approximately 60% (figure 1(c)), but is reduced to a few per cent when taking oxidation into account. Below 17 nm, the transmission is close to zero, which gives an explanation of the fast decrease of signal observed in the following spectra.

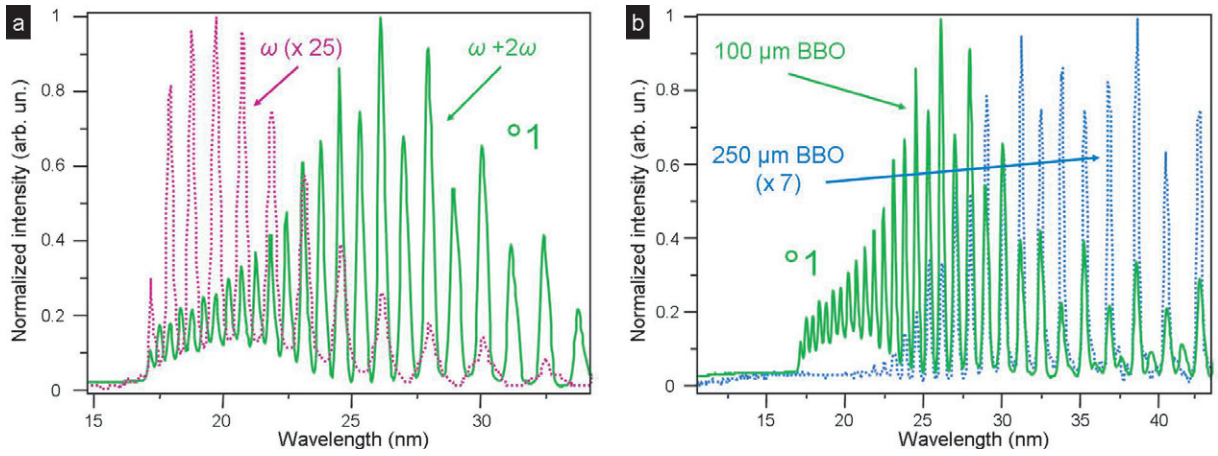

Figure 2. Normalized intensity HH spectra obtained with neon gas with either ω or $\omega + 2\omega$ technique and with the same optimization parameters as for ω: $E_\omega = 6\,\text{mJ}$, $\phi = 40\,\text{mm}$, $L_C = 7\,\text{mm}$ and $P_G = 35\,\text{mbar}$. (a) ω ($I_\omega \approx 7 \times 10^{14}\,\text{W cm}^{-2}$) and $\omega + 2\omega$ (100 μm thick BBO crystal, $I_\omega \approx 4.5 \times 10^{14}\,\text{W cm}^{-2}$ and $I_{2\omega} \approx 3.4 \times 10^{14}\,\text{W cm}^{-2}$). (b) $\omega + 2\omega$ with either 100 or 250 μm thick BBO crystal ($I_\omega \approx 3.9 \times 10^{14}\,\text{W cm}^{-2}$ and $I_{2\omega} \approx 4.8 \times 10^{14}\,\text{W cm}^{-2}$). The curves which are presented several times in the different figures, are marked with a '°' symbol in order to be recognized.

3. Typical spectral and intensity evolutions

The relatively high energy provided by our kHz IR laser allowed detailed study of a high repetition rate harmonic generation source with two-colour mixing in many gases. The IR peak power densities (I_{Laser}) required for the ionization of xenon, krypton, argon, neon and helium (I_P, the ionization potentials of atoms) are 0.7, 1, 2, 4 and $7 \times 10^{14}\,\text{W cm}^{-2}$, respectively. For any type of gas, two-colour effects are visible, and consist of three significant evolutions. The spectra for krypton are not presented in the paper in order to clarify the figures and the text, as its emission spectral region is fully covered by the ones of Ar and Xe. Figure 2, which presents the normalized intensity spectra obtained with Ne and with either the ω or $\omega + 2\omega$ technique, illustrates these three issues here.

Firstly, the harmonic content is doubled. Compared to classical harmonic generation, in which only odd orders of the fundamental frequency are produced, here even orders are also present: both $2 \times (2n + 1)$ components, the odd harmonics naturally generated by 2ω, and $2 \times (2n)$ components, coming from the mixing itself, where n is an integer.

Secondly, there is a redshift of the whole spectrum, i.e. a shifting to lower harmonic orders of the cut-off, the region where the number of photons starts to decrease fast. In a standard harmonic generation process, the spectral energy position of the cut-off, $E_{\text{cut-off}}$ (equation (2)), is mainly determined by the maximum of energy gained by the tunnelled electrons, oscillating in the laser field. This energy is equal to $3.2U_P$, where U_P (equation (3)) is the ponderomotive potential.

$$E_{\text{cut-off}} = I_P + 3.2U_P, \tag{2}$$

$$U_P = I_{\text{Laser}}\lambda^2_{\text{Laser}}, \tag{3}$$

where λ_{Laser} is the wavelength of the laser that generates the harmonics.

In our mixing case, a first approach to explain the general behaviour would be to simply consider that the laser is neither the IR beam nor the blue beam, but a 'mixed' beam, whose intensity and wavelength are bounded by the ω and 2ω ones. As a consequence, with the presence of the 2ω element, the maximum of energy reached by the electrons is decreased, as U_P is squarely dependent on the wavelength of the laser. This implies an increase of the cut-off position in terms of wavelength.

To be more specific, the intensity and wavelength are balanced by the $\omega/2\omega$ ratio. As a proof, the redshift is clearly dependent on the BBO thickness (figure 2(b)). The higher the BBO efficiency, the stronger the 2ω component compared to the ω component and the longer the wavelength where the cut-off occurs. These effects can also be partially explained by the delay evolution between the two beams. Indeed, in our geometrical configuration, the blue component arrives faster and faster in the medium with longer BBO thickness, and as the harmonic production is mainly affected by the front part of the arriving pulses, the 2ω component grows compared to the ω one and the $\omega/2\omega$ ratio decreases again.

Thirdly, a high factor of increase is observed here (figure 2(a)) when keeping the same optimization parameters as for ω, such as the energy and the IR beam aperture (respectively E_ω and ϕ), the gas pressure (P_G) and the cell length (L_C). Spectra present a relatively flat distribution with an intensity ratio from odd to even harmonics close to one, and the intensification arises over the whole spectrum.

Also, this enhancement is clearly dependent on the considered gas (figure 3(a)), typically He ($\times\approx100$), Ne ($\times\approx25$), Ar ($\times\approx0.5$), Kr ($\times\approx0.5$) and Xe ($\times\approx0.5$). As in a two-colour harmonic generation arrangement, the increasing efficiency has been explained by a higher ionization rate [29]; it could also be stated that the lower the ionization rate in the traditional harmonic generation (helium and neon), the stronger the enhancement factor with the mixing. For gases typically rather efficient like argon, krypton and xenon and using the same optimization parameters as for ω, there could even be actually a decrease of the maximum harmonic signal by a factor of 2. However, as the spectral content is doubled (and as the harmonic spectral width is similar), the whole energy seems to be conserved.

Due to this gas type dependence, the effect of flux increase can significantly vary in the observed full spectral range. In other words, the high efficiency of this two-colour process at short wavelengths notably compensates the low efficiency of the classical harmonic generation in this range. Consequently, it extends the spectral region accessible for applications and seeding to shorter wavelengths (figure 3(a)).

Basically, compared to the standard reference of harmonic generation in Ar, the Ne signal obtained with the $\omega+2\omega$ technique is on the same order of intensity (figure 3(b)). Importantly, the enhancement of the Ne signal mainly occurs between 30 and 20 nm, where typically classical HH generated from an 800 nm laser has a nearly negligible intensity, as this spectral region is located after the cut-off of Ar gas and before the efficient spectral range of Ne. Even more, accounting for the Al filter behaviour below 17 nm (transmission about 10^{-4}, figure 1(c)) and extrapolating the extension of the intensity decrease trend (figure 3(a)), it appears that a strong signal at 13 nm could have been extracted by using zirconium filters, whose transmission is quite important below 20 nm, instead of by using aluminium filters.

In summary, we observed here that using different harmonic generation techniques (either $\omega+2\omega$ or ω only), BBO thicknesses, and types of gas, an almost constant HH signal could be achieved from 65 to 13 nm. Besides, the required fine tuneability between one harmonic and another, which can be satisfied using either frequency-mixing [32] or laser chirp [33, 34]

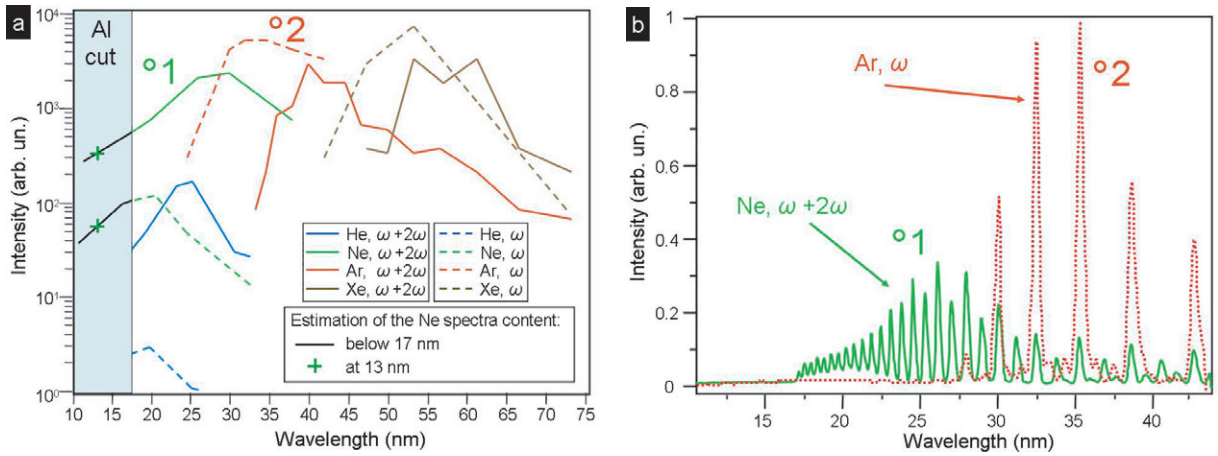

Figure 3. Intensity HH spectra obtained with either ω or $\omega+2\omega$ technique (100 μm thick BBO crystal) and with same optimization parameters as for ω: $E_\omega = 6$ mJ, $L_C = 7$–9 mm and $P_G = 30$–35 mbar. Xe and Ar cases: $\phi = 20$ mm, $I_\omega \approx 1.2 \times 10^{14}$ W cm^{-2} for ω configuration, and $I_\omega \approx 0.78 \times 10^{14}$ W cm^{-2}, $I_{2\omega} \approx 0.59 \times 10^{14}$ W cm^{-2} for $\omega+2\omega$ configuration. Ne and He cases: $\phi = 40$ mm, $I_\omega \approx 7 \times 10^{14}$ W cm^{-2} for ω configuration, and $I_\omega \approx 4.5 \times 10^{14}$ W cm^{-2}, $I_{2\omega} \approx 3.4 \times 10^{14}$ W cm^{-2} for $\omega+2\omega$ configuration. (a) Schematic representation of the achieved experimental intensity for different gases with both techniques (logarithmic scale). The presented curves match the fitted envelope of the recorded spectra. The light-blue window corresponds to the spectral part where the aluminium transmission is about 10^{-4}. Then, the black line represents the extrapolation of the extension of the intensity decrease trend below 17 nm. The green cross symbols show the corresponding estimations of the 13 nm signal. (b) Zoom of (a) around 30 nm. Ne with $\omega+2\omega$ and Ar with ω (linear scale). The curves which are presented several times in the different figures are marked with a '°' symbol in order to be recognized.

techniques, is two times smaller, due to the double harmonic content. Also, for higher orders, the needed tuneability is less important as harmonics start to dominate. A two-colour harmonic generation experiment using sub-10 fs IR laser [35] has even been demonstrated with argon gas a continuum of radiations from 25 to 33 nm, equivalent to the distance between four odd harmonics in the standard scheme using a typical 20–35 fs FWHM IR laser. Thus, the two-colour harmonic generation scheme is an appropriate solution for seeding PSXL and FEL in this very large spectral range, and furthermore it would allow the FEL tuneability to be maintained.

4. Optimization of the flux

Since the two-colour harmonic generation process is different from the standard one at the fundamental frequency (short electron path selection and higher ionization rate), the optimal parameters for the two cases have to be notably different. Actually, it even corresponds to quite drastic changes. For instance, figure 4 presents the Ar example. For optimizing the HH flux, both

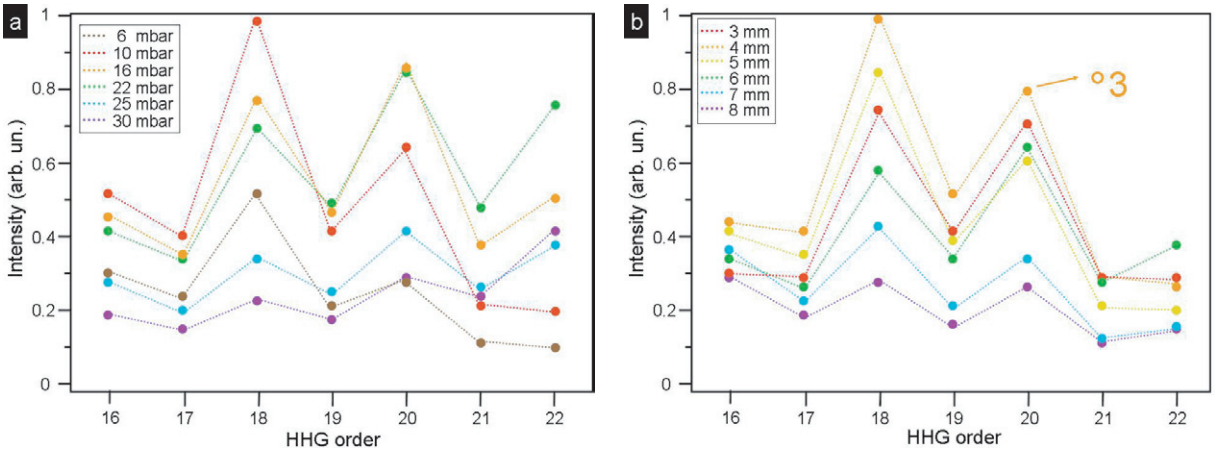

Figure 4. Representation of the intensity maxima (dot symbols) of the HH orders obtained in Ar with the $\omega+2\omega$ technique (100 μm thick BBO crystal), full aperture beam ($\phi = 40$ mm) and $E_\omega = 5.2$ mJ. $I_\omega \approx 3.9 \times 10^{14}$ W cm^{-2}, $I_{2\omega} \approx 2.9 \times 10^{14}$ W cm^{-2}. The curves correspond to the fitted envelope of the recorded spectra. (a) Variation of the gas pressure in a 6 mm long gas cell. (b) Variation of the cell length under constant pressure of 16 mbar. The curves which are presented several times in the different figures are marked with a '$\circ$' symbol in order to be recognized.

the gas pressure and the cell length are approximately two times smaller, respectively, from 30 to 16 mbar and 8 to 4 mm.

The recorded spectrum resulting from these optimal mixing parameters is plotted in figure 5(a) in order to be compared to the classical harmonic generation one. It shows that even with a gas like argon, which is relatively efficient in the classical harmonic generation, a reasonable enhancement can be obtained (factor of 2), as lower pressure and smaller propagation length in the cell involve in the case of argon smaller absorption in the 40–70 nm range. Spectra from figure 4 also reveal that the magnification mainly occurs for some particular orders, i.e. for both types of even orders. Especially, the most visible evolution stands for the 18th and 20th orders corresponding to 44 and 40 nm.

In addition to the gas pressure and cell length optimization, stronger enhancement is reached when increasing the laser energy for generation, i.e. by directly increasing the available energy at the exit of the compressor (E_ω) and/or by opening the iris aperture further (ϕ). With the best optimization case, an enhancement factor of the HH yield equal to 20 is then observed compared to the classical harmonic generation (blue curve of figure 5(b) and red curve of figure 5(a)). However, the intensification essentially takes place in the $2 \times (2n+1)$ components of the even orders (figure 5(b)), while complementary components saturate ($2 \times (2n)$). These $2 \times (2n+1)$ components are the orders that can be generated by the 2ω component alone, whose intensity is stronger now. Indeed, higher laser energy leads to higher conversion in the crystal and still even higher blue intensity as the focal spot is smaller than the IR one.

This clearly means that in a two-colour field harmonic generation configuration, both IR and blue beams have to be intense to reach the highest HH yield and as a consequence higher laser energy than in a single-colour configuration is required. This is why, as in our current

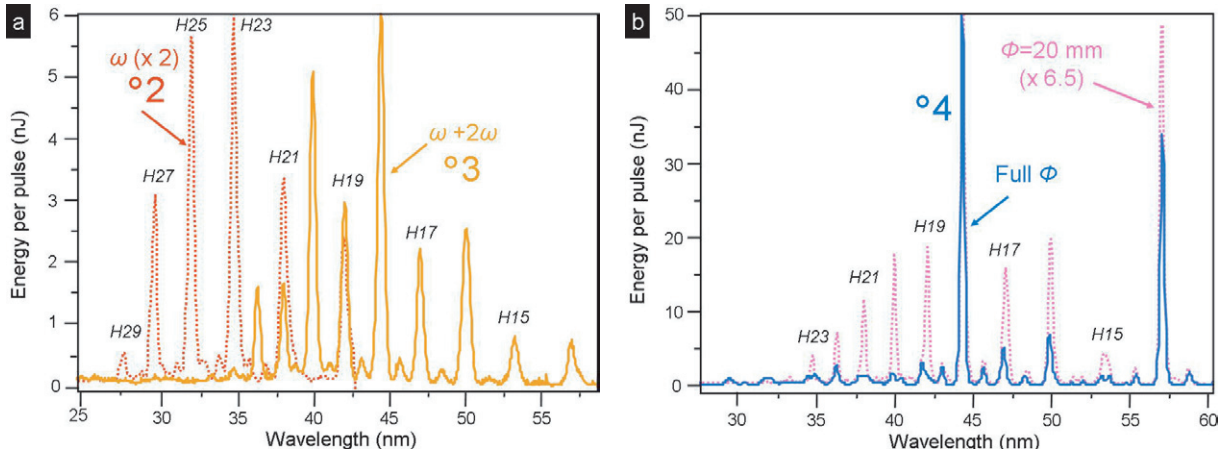

Figure 5. HH spectra calibrated in energy per pulse and obtained in Ar with either ω ($L_C = 8$ mm and $P_G = 30$ mbar) or $\omega + 2\omega$ (100 μm thick BBO crystal, $L_C = 4$ mm and $P_G = 16$ mbar) technique, for different laser energies and iris apertures. H14 to H29 correspond to the harmonic orders. (a) Full aperture beam ($\phi = 40$ mm). $E_\omega = 6$ mJ, $I_\omega \approx 1.2 \times 10^{14}$ W cm^{-2} for ω configuration and $E_\omega = 5.2$ mJ, $I_\omega \approx 3.9 \times 10^{14}$ W cm^{-2}, $I_{2\omega} \approx 2.9 \times 10^{14}$ W cm^{-2} for $\omega + 2\omega$ configuration. (b) $\omega + 2\omega$, $E_\omega = 6.8$ mJ and either $\phi = 40$ mm ($I_\omega \approx 4.4 \times 10^{14}$ W cm^{-2}, $I_{2\omega} \approx 5.4 \times 10^{14}$ W cm^{-2}) or $\phi = 20$ mm ($I_\omega \approx 0.77 \times 10^{14}$ W cm^{-2}, $I_{2\omega} \approx 0.94 \times 10^{14}$ W cm^{-2}). The curves which are presented several times in the different figures are marked with a '°' symbol in order to be recognized.

harmonic generation geometry, the intensity is limited by a rather long focal length lens (1.5 m), such an additional effect of yield enhancement on the $2 \times (2n + 1)$ components of the even orders could not have been observed for gases like He and Ne for which ionization potentials are higher than for Ar, Kr and Xe.

The significant drawback of the whole optimization method, aiming at maximizing the harmonics flux generated in the mixing, is the induced strong redshift. Indeed, as the gas pressure decreases (figure 4(a)) and as the laser energy increases (figure 5(b)), the harmonics shift to lower orders. This also comes from the higher blue component taking part in the generation process (equations (2) and (3)) in that case. Indeed, this explains both the strong redshift and the enhancement of the $2 \times (2n + 1)$ orders first observed by the role of the iris aperture and laser energy scaling (figure 5(b)) and is confirmed by the observation of similar effects when using lower laser energy but a thicker BBO crystal (250 μm, not shown here), giving in all cases a higher blue component. Moreover, the whole behaviour exactly corresponds to that suggested by simulations performed with neon gas in [29] with variable 2ω intensity.

To finally quantify more clearly the HH yield, the energy per pulse has been calibrated in absolute with the solarblind photodiode. It leads to a quite similar result to calculating the global efficiency of the spectrometer and taking into account the experimental filter transmission ($\approx$5%) and theoretical spherical mirror reflectivity ($\approx$75%). In our two-colour arrangement, the maximum number of photons per shot reached with Ar gas is about 10^{10} at 44 nm and corresponds to 50 nJ (figure 5(b), figure 6). As previously mentioned, in

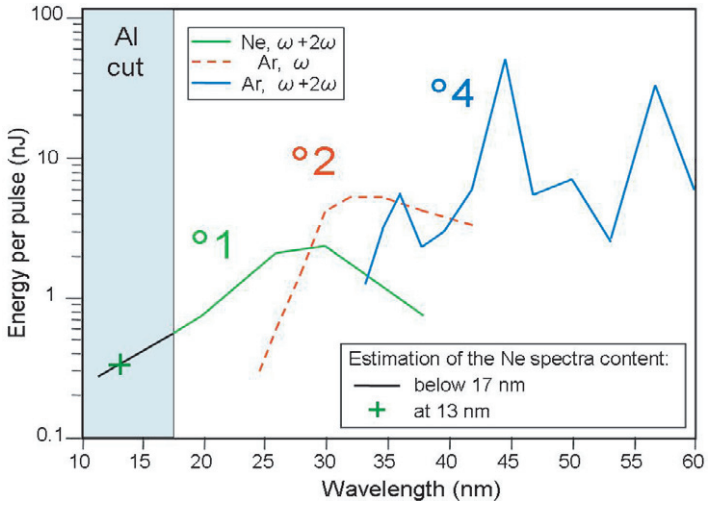

Figure 6. Schematic representation in the spectral window adapted for the seeding of the highest experimental HH energies per pulse achieved in various conditions (logarithmic scale). The light-blue window corresponds to the spectral part where the aluminium transmission is about 10^{-4}. Then, the black line represents the extrapolation of the extension of the intensity decrease curvature below 17 nm. The green cross symbols show the corresponding estimations of the 13 nm signal. ω: typical Ar reference ($\phi = 20$ mm, $I_\omega \approx 1.2 \times 10^{14}$ W cm^{-2}). $\omega + 2\omega$: Ne ($\phi = 20$ mm, $I_\omega \approx 4.5 \times 10^{14}$ W cm^{-2}, $I_{2\omega} \approx 3.4 \times 10^{14}$ W cm^{-2}) and Ar ($\phi = 40$ mm, $I_\omega \approx 4.4 \times 10^{14}$ W cm^{-2}, $I_{2\omega} \approx 5.4 \times 10^{14}$ W cm^{-2}). The curves which are presented several times in the different figures are marked with a '°' symbol in order to be recognized.

such a rather long focusing geometry, the intensity of the fundamental and second harmonic is not high enough in the case of He and Ne gases. This is why with a slightly higher energy laser, one can expect to get harmonics from Ne, particularly the $2 \times (2n + 1)$ components of the even orders, with almost one order of magnitude higher energy per pulse than measured here.

5. A source for seeding FEL or PSXL

Suitable and, above all, intense HH sources are urgently needed in the VUV to the soft x-ray region for seeding. In an FEL, first a non negligible seed intensity is required to overcome the shot noise of the electron beam, which grows stronger at shorter wavelengths, and second a high intensity seed helps to obtain saturation in a more compact system [8]. Although PSXL seeding has already been performed below 30 nm, the injected seed energies were so limited (tens of picojoules) that the amplified beam energies did not attain more than 100 nJ [3, 5, 6]. This is why the $\omega + 2\omega$ technique applied for the seeding of FEL and PSXL is very promising.

For example, in the present two-colour experiment, three wavelength regions suitable for seeding are emphasized, around 44 nm, from 26 to 18 nm and 13 nm, in which harmonic yields are compared in terms of intensity to the classical Ar reference with ω only at 32–35 nm. Table 1 summarizes, in particular, the values of the energy per pulse which have been experimentally measured ($E_{\mathrm{HH,meas.}}$) in our kHz two-colour harmonic generation setup (figure 6): 50 nJ at 44 nm, 2.5 nJ at 26 nm, 0.65 nJ at 18 nm and 0.3 nJ at 13 nm while 5 nJ is reached for the reference.

Table 1. Summary of harmonics energy per pulse at the generation point, coming from either experimental measurements in the current setup ($E_{\mathrm{HH,meas.}}$), or from estimations in a long focal geometry setup ($E_{\mathrm{HH,l.f.}}$). $E_{\mathrm{inj.,l.f.}}$ corresponds to the real injected energy per pulse (i.e. after the seeding optics) 'seen' by the amplification medium and which could be obtained in the long focal geometry.

Technique	Gas type	λ (nm)	$E_{\mathrm{HH,meas.}}$ (nJ)	$E_{\mathrm{HH,l.f.}}$ (nJ)	$E_{\mathrm{inj.,l.f.}}$ (nJ)
ω (reference)	Ar	32–35	5	500	50
$\omega + 2\omega$	Ar	44	50	5000	500
$\omega + 2\omega$	Ne	26	2.5	250	25
$\omega + 2\omega$	Ne	18	0.65	65	6.5
$\omega + 2\omega$	Ne	13	≈0.3	≈30	≈3

For the seeding of FEL, these energy levels are delicate; such measured values are basically high enough down to 20 nm but not for shorter wavelengths due to technical and physics issues. Firstly, as an efficient spatial overlap is required between either the electron beam bunches and the seed, appropriate optics, which softly attenuate the seed energy, have to be added in order to control the refocusing and the alignment of the HH beam in the electron medium. Using a restricted number of grazing incidence reflective optics, this reduction will be limited most likely to less than one order of magnitude. Secondly, the injected peak power must overcome the electron beam shot noise, which is inversely proportional to the wavelength of emission, and which is as a consequence rather high at wavelengths lower than 20 nm, while the HH seed energy starts to decrease fast (figure 6).

The solution could come from the combination of the two-colour scheme with an additional well-known harmonic generation technique allowing the increasing of the harmonics flux. Indeed, with higher laser energy and longer focal length geometry (5–7 m), the general high harmonic efficiency could be enhanced; a typical energy per pulse of around 500 nJ at 32–35 nm could be engaged for [36]. Consequently, coupling such a focusing geometry to a $\omega + 2\omega$ setup would allow photons with 5 μJ energy per pulse to be generated at 44 nm, 250 nJ at 26 nm, 65 nJ at 18 nm and about 30 nJ at 13 nm (table 1, $E_{\mathrm{HH,l.f.}}$). Maintaining the conservative value of global transmission for the seeding optics, the real energies per pulse available for seeding would be in that case: 0.5 μJ at 44 nm, 25 nJ at 26 nm, 6.5 nJ at 18 nm and 3 nJ at 13 nm (table 1, $E_{\mathrm{inj.,l.f.}}$).

Following [25], in order to overcome the electron beam shot noise in the 44–13 nm (maximum of 10 W peak power at 13 nm) region, and observe fully coherent FEL emission, the seed energy (for a 50 fs FWHM pulse duration) must be close to 1 nJ = 50 fs × 10 W × 200 (factor for coherent amplification) ×10 (spatial overlap with the electron beam). Therefore, seeding down to 13 nm, as scheduled by the sFLASH team, is clearly feasible with the implementation of a two-colour setup in a long focal geometry, and which could deliver 3 nJ in the active medium. According to figures 3(a) and 6, this should not be obtained with a standard HH setup for Ne gas, as the real energy per pulse at 13 nm would be restricted to approximately 0.05 nJ (about 6.5 times lower than that obtained with $\omega + 2\omega$, i.e. 0.3 nJ). Basically, in classical harmonic generation the shortest wavelength accessible for observing coherent amplification in FEL seeding is about 30 nm using Ar gas.

These levels of energy are relatively important for other applications in general and suitable for seeding experiments of PSXL down to 18 nm, which do not require very high seed intensity.

Indeed, the injected beam must overcome rather weak levels of ASE, whose amplitudes are not really sensitive to the wavelength of the emission. Saturated emission in seeding configuration has been first observed while the seed energy was equal to 35 nJ at 32.8 nm [1]. But 0.35 nJ was enough in the same installation for getting high amplification in a well-defined spatial mode. Then at 18.9 nm only 0.2 nJ [5] to 1 nJ [3] allowed one to obtain a strong amplification factor ($\times$400).

A number of PSXL could then benefit from the elevated harmonic flux, especially in the 26–18 nm region: Ne-like Ni (23.14 nm), Se (20.5 nm) and Ge (19.63 nm), Ni-like Y (24.03 nm), Zr (22.07 nm) and Nb (20.47 nm). Indeed, even in our relatively short focusing geometry system (1.5 m) and with a conservative reduction factor of 10 for the HH propagation to the plasma, the available seed energy per pulse around 18 nm reaches 65 pJ (0.65 nJ/10, table 1), which is of the order of the value reported with a 5 m long focal lens in the Ni-like Mo seeding experiment ($<$0.2 nJ) [5]. As a consequence, combination with long focal geometry would lead to the use of larger plasmas and/or shorter amplification lengths in order to reach the saturation faster and possibly also extracting more energy, leading to an unprecedented high peak spectral brightness close to the FEL one. Seeding experiments at 13 nm, which have been developed thanks to very high reflective optics for lithography, could easily be realized for instance in the Ni-like Ag (13.9 nm) and the Ni-like Cd (13.2 nm). Even at shorter wavelengths, the seed energy would be kept large enough to observe amplification ($<$3 nJ, $E_{\mathrm{inj.,l.f.}}$, table 1). Finally, the critical spectral overlap, which requires drastic changes of the laser chirp (leading to lower HH efficiency and larger pulse durations) as the wavelength of emission of a PSXL is fixed (contrary to FEL devices), is easier to perform in a two-colour harmonic generation configuration due to the double harmonic content.

Seeding could also help to saturate the FEL signal at shorter wavelengths than in the SASE mode (figure 7). For instance, the SCSS Test Accelerator delivers a certain photon flux from 30 nm to more than 60 nm [11], but the full saturation only occurs starting from 55 nm. At 44 nm, the FEL intensity is reduced by a factor of 20, far from the saturation, which increases the shot to shot instability by 3 to about 30%. Figure 7 presents simulated evolutions, performed with the 1D code Perseo Time Dependent [37], of the peak power in the 9 m long FEL amplification device, the undulator.

It shows that full saturation is obtained at 44 nm in seeding configuration while the HH seed peak power is employed (based on our experimental results); 150 kW corresponding to 5 nJ energy (50 nJ measured at 44 nm with the one order of magnitude reduction factor accounting for global transmission of seeding optics) in a 35 fs FWHM pulse is restrained in such a condition of short focal lens geometry. But, more than getting higher flux at a shorter wavelength, seeding with HH also aims at improving the spectral and intensity stabilities. If the first one has been well established [38], the second one is more challenging as the sources of instability implying that FEL shot to shot intensity variations are diverse in the seeding scheme, such as the intensity and the wavelength of emission of the harmonic pulses, and the temporal and spatial overlaps with the electron beam. Among these, the main technical issue is the required femtosecond synchronization. But if this is achieved, then the major component of instability is the seed intensity fluctuation, which is directly linked to the high nonlinearity of the harmonic generation process and as a consequence is difficult to keep small. In special conditions of relatively long electron beam pulses, like the case of the SCSS Test Accelerator (1 ps FWHM), and with the usual 50 fs of temporal jitter standing for a HH pulse of 35 fs (FWHM), the induced intensity fluctuations would be quite small, 2.6%.

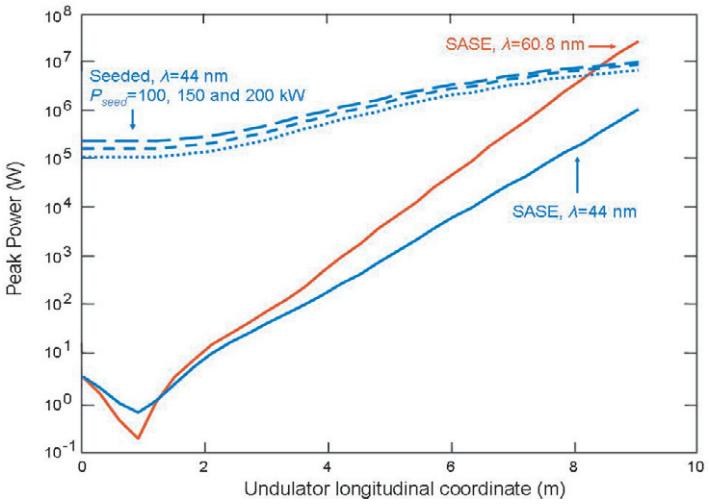

Figure 7. Simulated evolution of the FEL peak power signal as a function of the amplification device (undulator) length in SASE (classical mode) and seeding configurations with harmonics for fundamental radiated wavelengths (λ) of 60.8 nm and 44 nm. The calculations have been made using the Perseo Time Dependent code with the following parameters from [11]. Electron beam parameters: (energy) $E = 250$ MeV, (slice energy spread) $\sigma_E = 3 \times 10^{-4}$, (peak current) $I = 300$ A, (charge) $q = 0.32$ nC and (slice emittance) $\epsilon = 0.7$ mm mrad. Undulator parameters: (spatial period) $\lambda_U = 15$ mm, (number of periods) $N = 2 \times 300$, (deflection parameter) $K_{60.8\,nm} = 1.37$ or $K_{44\,nm} = 0.9$. Seed parameters: (seeding wavelength) $\lambda_{seed} = 44.09$ nm, (peak power) $P_{seed} = 150\,kW \pm 33\%$, (pulse duration) $\tau = 35$ fs FWHM. For $P_{seed} = 100$ kW, the temporal centroid positions of the HH pulse and electron bunch are shifted by 50 fs.

Furthermore, even when adding relatively strong harmonic intensity variations, typically 30%, variations would remain smaller than in the best SASE conditions, i.e. less than 10% (figure 7, $P_{seed} = 150\,kW \pm 33\%$).

Finally, in combination with the possibility of controlling the high harmonic spectra with the two-colour technique (regulation of the injected amount of seed at the desired wavelength), seeding will provide users with a quite stable light, not only at the designed FEL wavelength, but within a much larger range towards the soft x-ray region. This experimental proposal is obviously applicable for other future FEL devices for generating SASE light in the soft x-ray region as long as a strong harmonic signal is produced, which overcomes the shot noise.

6. Conclusions and perspectives

The two-colour scheme, implemented on our kHz HH line, has allowed us to extensively study both spectral and intensity evolutions of the double content harmonic spectra, with typical parameters such as the type of gas, the gas pressure, the cell length as well as the intensity of the 400 nm component. It has been shown that either a limited magnification of the whole spectrum is obtained with optimization parameters close to the ω ones, a more significant increase of

both types of even harmonics with twice smaller cell length and gas pressure, or finally a very strong enhancement is mainly located on the $2 \times (2n+1)$ components due to a higher 400 nm component. Nevertheless, this final step occurs at higher wavelengths. This is why the adaptation of the $\omega + 2\omega$ technique for seeding experiments requires a strong control of the generation, in order to keep the redshift effect small but still obtain as many photons as possible at the selected wavelength. As pointed out before, in our current very simple $\omega + 2\omega$ setup with BBO crystal directly in the laser path, the IR and blue components are slightly delayed due to the group delay dispersion difference, which prevent BBO crystals thicker than 250 μm being used. Moreover, the intensity ratio of these two pulses cannot be well adjusted as changing the energy of the laser beam directly affects the blue one. These issues could be solved with two separate lines for ω and 2ω [39], which are then recombined in the gas medium. Yet, in that case the spatial matching of the two beams would be more delicate.

Basically, the two-colour harmonic generation configuration brought very promising results for seeding FEL or PSXL in the VUV to the soft x-ray domain. Indeed, as this method was here revealed to be more and more efficient at shorter wavelengths, it significantly compensates the standard harmonic generation performance, giving an almost constant number of photons in this range, and as a consequence seeding at shorter wavelengths than previously accessible can be envisaged. In addition, the evidence of the strong enhancement in argon on the $2 \times (2n+1)$ components, and especially at 44 nm, associated with the possibility to control the spectra could, for instance, serve to extend the SCSS Test Accelerator FEL saturation to shorter wavelengths and deliver more stable light for applications. Finally, the strong HH strengthening demonstrated in the 27–13 nm range is an essential result for the future soft x-ray seeded FEL sFLASH, and also for the tremendous number of PSXL available in this range.

To conclude, in order to attain x-ray radiation (from 10 to 0.01 nm), the use of higher fundamental wavelength lasers, such as parametric amplifiers (1.2–1.5 μm [26]), is foreseen. Indeed, according to equations (2) and (3), this would correspond to a strong blueshift of the cut-off region. Coupled to the two-colour strong yield increasing effect observed in Ne or He gases, intense HH pulses could be generated in such a spectral region for both FEL and PSXL seeding. The so-called water-window ($\approx$2–4 nm), of interest for the study of biological samples, and perhaps even the Angström region (0.1 nm) could be then reached.

Acknowledgments

CPH acknowledges support from the Laserlab Integrated Infrastructures Initiative RII-CT-2003-506350. Financial support for this work was provided by the TUIXS European project (Table top Ultra Intense XUV Sources) FP6 NEST-Adventure n.012843.

References

[1] Zeitoun P *et al* 2004 *Nature* **431** 426
[2] Kawachi T *et al* 2005 *Proc. JAERI* vol 1 (Bellingham, WA: International Society for Optical Engineering) p 5919
[3] Wang Y *et al* 2006 *Phys. Rev. Lett.* **97** 3901
[4] Goddet J-Ph *et al* 2007 *Opt. Lett.* **32** 1498–1500
[5] Wang Y *et al* 2008 *Nat. Photonics* **2** 94
[6] Pedaci F *et al* 2008 *Opt. Lett.* **33** 491–3

[7] McNeil B W J *et al* 2007 *New J. Phys.* **9** 82
[8] Lambert G *et al* 2008 *Nat. Phys.* **889** 296
[9] Salières P, L'Huillier A and Lewenstein M 1995 *Phys. Rev. Lett.* **74** 3776
[10] Le Déroff L *et al* 2000 *Phys. Rev.* A **61** 043802
[11] Shintake T *et al* 2008 *Nat. Photonics* **2** 555
[12] Labat M *et al* 2007 *Nucl. Instrum. Methods Phys. Res.* A **593** 26
[13] Schlarb H *et al* 2007 *Proc. FEL'07 Conf.* vol 1 (JACOW) p 211
[14] Tiedtke K *et al* 2009 *New J. Phys.* **11** 023029
[15] http://www.elettra.trieste.it/FERMI/
[16] Brandin M *et al* 2008 *J. Phys.: Conf. Ser.* **100** 022001
[17] http://www.sparx-fel.it/
[18] Couprie M-E *et al* 2008 *Proc. EPAC'08 Conf.* vol 1 (JACOW) p 73
[19] Reiche S 2008 *Workshop Lausanne*
[20] Yu L H *et al* 2000 *Science* **289** 932
[21] Dattoli G and Ottaviani P L 1999 *J. Appl. Phys.* **86** 5331
[22] Giannessi L and Musumeci P 2006 *New J. Phys.* **8** 294
[23] Bonifacio R, Pellegrini C and Narducci L 1984 *Opt. Commun.* **50** 373
[24] Saldin E L, Schneidmiller E A and Yurkov M V 1998 *Opt. Commun.* **148** 383
[25] Lambert G *et al Phys. Rev. Lett.* submitted
[26] Shan B, Cavalieri A and Chang Z 2002 *Appl. Phys.* B **74** 23
[27] Watanabe S, Kondo K, Nabekawa Y, Sagisaka A and Kobayashi Y 1994 *Phys. Rev. Lett.* **73** 2692
[28] Kim I J, Lee G H, Park S B, Lee Y S, Kim T K and Nam C H 2008 *Appl. Phys. Lett.* **92** 021125
[29] Kim C M, Kim I J and Nam C H 2005 *Phys. Rev.* A **72** 033817
[30] http://www-cxro.lbl.gov/
[31] Kazamias S *et al* 2002 *Eur. Phys. J.* D **21** 353
[32] Eichmann H *et al* 1995 *Phys. Rev.* A **51** 3414
[33] Lee D G 2001 *Phys. Rev. Lett.* **87** 243902
[34] Mauritsson J *et al* 2004 *Phys. Rev.* A **70** 021801
[35] Oishi Y, Kaku M, Suda A, Kannari F and Midorikawa K 2006 *Opt. Express* **14** 7230
[36] Takahashi E, Nabekawa Y, Otsuka M and Midorikawa K 2002 *Phys. Rev.* A **66** 021802
[37] Giannessi L 2006 *Proc. FEL'06 Conf.* vol 1 (JACOW) p 91
[38] Hara T *et al* 2008 *Proc. FEL'08 Conf.* vol 1 (JACOW)
[39] Eichmann H *et al* 1995 *Phys. Rev.* A **51** R3414